



Molecular Mechanisms of Allosteric Inhibition of Brain Glycogen Phosphorylase by Neurotoxic Dithiocarbamate Chemicals

Cécile Mathieu, Linh-Chi Bui, Emile Petit, Iman Haddad, Onnik Agbulut, Joelle Vinh, Jean-Marie Dupret, Fernando Rodrigues-Lima

► To cite this version:

Cécile Mathieu, Linh-Chi Bui, Emile Petit, Iman Haddad, Onnik Agbulut, et al.. Molecular Mechanisms of Allosteric Inhibition of Brain Glycogen Phosphorylase by Neurotoxic Dithiocarbamate Chemicals. Journal of Biological Chemistry, 2017, 292 (5), pp.1603 - 1612. <10.1074/jbc.M116.766725>. <hal-01636517>

HAL Id: hal-01636517

<https://hal.science/hal-01636517v1>

Submitted on 29 Nov 2021

HAL is a multi-disciplinary open access archive for the deposit and dissemination of scientific research documents, whether they are published or not. The documents may come from teaching and research institutions in France or abroad, or from public or private research centers.

L'archive ouverte pluridisciplinaire **HAL**, est destinée au dépôt et à la diffusion de documents scientifiques de niveau recherche, publiés ou non, émanant des établissements d'enseignement et de recherche français ou étrangers, des laboratoires publics ou privés.



HAL Authorization

Molecular Mechanisms of Allosteric Inhibition of Brain Glycogen Phosphorylase by Neurotoxic Dithiocarbamate Chemicals^{*[5]}

Received for publication, November 7, 2016, and in revised form, December 8, 2016. Published, JBC Papers in Press, December 13, 2016, DOI 10.1074/jbc.M116.766725

Cécile Mathieu[‡], Linh-Chi Bui[‡], Emile Petit[‡], Iman Haddad[§], Onnik Agbulut[¶], Joelle Vinh[§], Jean-Marie Dupret^{¶||}, and Fernando Rodrigues-Lima^{‡||1}

From the [‡]Université Paris Diderot, Sorbonne Paris Cité, Unité BFA, CNRS UMR 8251, 75013 Paris, France, [§]ESPCI ParisTech, Université Paris Sciences et Lettres, Laboratoire de Spectrométrie de Masse Biologique et Protéomique, CNRS USR, 3149 Paris, France, the [¶]Sorbonne Universités, UPMC Univ Paris 06, Institut de Biologie Paris-Seine, UMR CNRS 8256, Biological Adaptation and Ageing, 75005 Paris, France, and ^{||}UFR Sciences du Vivant, Université Paris Diderot, 75013 Paris, France

Edited by Ruma Banerjee

Dithiocarbamates (DTCs) are important industrial chemicals used extensively as pesticides and in a variety of therapeutic applications. However, they have also been associated with neurotoxic effects and in particular with the development of Parkinson-like neuropathy. Although different pathways and enzymes (such as ubiquitin ligases or the proteasome) have been identified as potential targets of DTCs in the brain, the molecular mechanisms underlying their neurotoxicity remain poorly understood. There is increasing evidence that alteration of glycogen metabolism in the brain contributes to neurodegenerative processes. Interestingly, recent studies with *N,N*-diethyldithiocarbamate suggest that brain glycogen phosphorylase (bGP) and glycogen metabolism could be altered by DTCs. Here, we provide molecular and mechanistic evidence that bGP is a target of DTCs. To examine this system, we first tested thiram, a DTC pesticide known to display neurotoxic effects, observing that it can react rapidly with bGP and readily inhibits its glycogenolytic activity ($k_{\text{inact}} = 1.4 \times 10^5 \text{ M}^{-1} \text{ s}^{-1}$). Using cysteine chemical labeling, mass spectrometry, and site-directed mutagenesis approaches, we show that thiram (and certain of its metabolites) alters the activity of bGP through the formation of an intramolecular disulfide bond (Cys³¹⁸–Cys³²⁶), known to act as a redox switch that precludes the allosteric activation of bGP by AMP. Given the key role of glycogen metabolism in brain functions and neurodegeneration, impairment of the glycogenolytic activity of bGP by DTCs such as thiram may be a new mechanism by which certain DTCs exert their neurotoxic effects.

Dithiocarbamates (DTCs)² are organosulfur compounds widely used as fungicides for agricultural products. They are

used in industrial settings as an accelerating agent and have therapeutic applications in alcoholic aversion therapy (1). However, the wide use of this large family of chemicals has raised many issues concerning their impact on human health. For instance, the DTC pesticide thiram has been reported to display neuropathic effects and is associated with the development of a Parkinson's disease-like syndrome (2, 3). DTCs and some of their metabolites are highly reactive electrophilic compounds that can react with biological macromolecules through covalent modification of cysteine residues. In particular, DTC compounds have been shown to form mixed disulfides and/or to induce the formation of disulfide bonds in proteins, peptides, or enzymes that can modulate their biological activities (1, 4). Although neuropathy induced by DTCs is a major toxic effect that has been reported by several studies in humans and animals (2, 3, 5, 6), the molecular mechanisms underlying the neurotoxicity of DTCs are not well understood. Impaired ubiquitin activation, stimulation of non-selective cation channels, changes in membrane potential, and alteration of ATP-dependent uptake of glutamate have been shown to contribute to the neurotoxic effects of DTCs (7–9). Enzymes such as proteasome, ubiquitin-activating enzyme E1, or peptidoglycine-5 hydroxylating monooxygenase have been shown to be inhibited by DTCs in the brain (10–12).

Glycogen is the main carbohydrate store of glucose in mammalian cells. In the brain, glycogen is predominantly found in astrocytes and to a lesser extent in the neurons (13–15). In the past years, a new interest was given to brain glycogen because it participates in several neurological processes, providing energy and substrates to brain cells and sustaining high cognitive processes including learning and memory consolidation (16–18). In addition, astrocytic and neuronal glycogen provides protection to neurons and promotes their survival under stress conditions such as hypoglycemia and hypoxic stress (15, 19, 20). However, although brain functions and brain cell survival critically rely on the brain glycogen store, the accumulation of glycogen is toxic for cells and is a direct cause of neurodegeneration in the brain (21). Glycogen phosphorylase (GP) is the key enzyme for glycogen mobilization. In humans, this enzyme exists as three isoforms named after the tissue where they are mainly expressed: the muscle GP, the liver GP, and the brain GP

^{*} This work was supported by University Paris Diderot, CNRS, and a Ph. D. fellowship from University Paris Diderot (Ecole Doctorale BioSPC; to C. M.). The authors declare that they have no conflicts of interest with the contents of this article.

^[5] This article contains supplemental Tables S1 and S2 and Fig. S1.

¹ To whom correspondence should be addressed. E-mail: fernando.rodrigues-lima@univ-paris-diderot.fr.

² The abbreviations used are: DTC, dithiocarbamate; DEDC, *N,N*-diethyldithiocarbamate; GP, glycogen phosphorylase; bGP, brain GP; 5-IAF, 5-iodoacetamide-fluorescein; DMDC, dimethyldithiocarbamate; NEM, *N*-ethylmaleimide; CAM, carbamidomethyl.

This is an Open Access article under the CC BY license.

Dithiocarbamate Inhibition of Brain Glycogen Phosphorylase

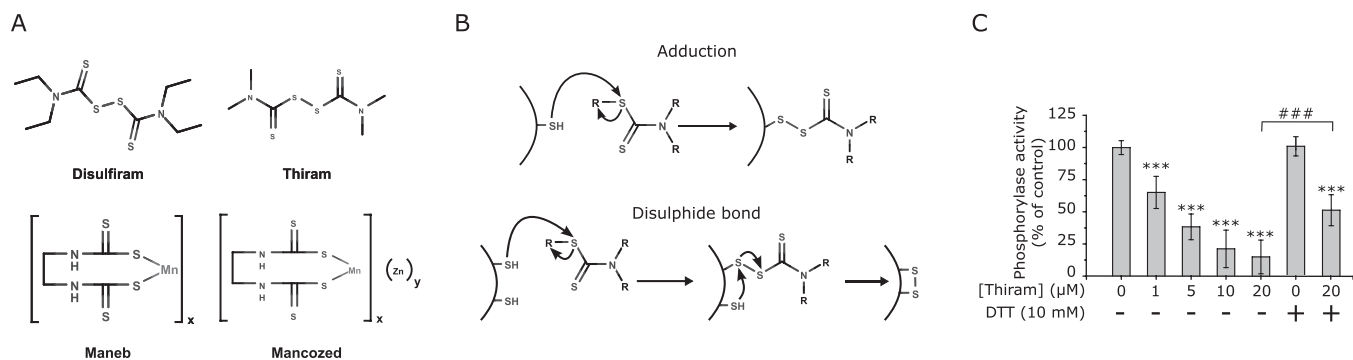


FIGURE 1. *A*, the chemical structure of parent DTC compounds tested. Several DTCs were tested for inhibition of the bGP. Disulfiram and thiram are oxidized DTCs widely used in therapeutics and as pesticides, respectively. Mancozeb and maneb are model DTCs found in complex with ions. *B*, schematic representation of the reactivity of DTCs. DTCs interact with the thiol groups of cysteine residues, leading to the formation of an adduct (*upper panel*) and/or the formation of an intramolecular disulfide bond (*lower panel*) with a vicinal cysteine. *C*, phosphorylase activity is irreversibly altered in brain extracts exposed to thiram. Mice brain extracts were exposed to increasing concentrations (0–20 μM) of thiram for 30 min prior to activity measurement. To investigate the ability of reducing agent to restore GP activity, brain extracts exposed to thiram were further incubated with 5 mM DTT for 10 min, and activity was measured. GP activity is expressed as percentages of the positive control. The data represent mean values of three independent experiments ± S.D. ***, $p < 0.001$ compared with control; ###, $p < 0.001$ when two groups are compared.

(bGP). These enzymes are regulated by both the binding of allosteric effectors (including AMP and ATP) and phosphorylation, in response to local or extracellular energy needs (22). Moreover, the activity of bGP can be redox-regulated through the formation of an intramolecular disulfide bond between Cys³¹⁸ and Cys³²⁶, which controls the AMP-dependent activation of this GP isozyme. Together, these tight regulations of bGP enzyme may participate to control of glycogen metabolism in the brain (23).

Recent studies with *N,N*-diethyldithiocarbamate (DEDIC) suggest that bGP and glycogen metabolism could also be altered by DTCs (7). To better understand the molecular mechanisms underlying the neurotoxic effects of DTCs, we investigated the potential molecular and functional effects of a neurotoxic DTC pesticide thiram, on bGP. We found that thiram (and certain of its metabolites), inhibited bGP through the formation of an intramolecular disulfide bond between Cys³¹⁸ and Cys³²⁶, two residues involved in the redox regulation of bGP (23). Altogether, our results suggest that the modulation of bGP activity by DTCs may participate in the neurotoxic effects of these chemicals.

Results

bGP Is Inhibited in Brain Extracts Treated with Thiram—DTCs (Fig. 1A) are chemicals known to directly modify proteins through the covalent adduction of cysteine residues and/or the formation of disulfide bonds (Fig. 1B). In addition, DTCs can also be metabolized to certain reactive oxidative metabolites that irreversibly or reversibly modulate protein functions via the covalent modification of cysteine residues (1, 7, 24). Rat models and recent proteomic studies suggested that brain glycogen phosphorylase is a putative target of DTC chemicals in the brain (7). In addition, this isoenzyme has been described as presenting highly reactive cysteine residues (23, 25–27). To further determine the impact of DTCs on bGP activity and glycogen metabolism in the brain, we treated mice brain extracts with thiram (Fig. 1A), a well known neurotoxic DTC pesticide, using concentrations (0–20 μM) previously employed in toxicological *in vitro* models (8, 9). As shown in Fig. 1C, thiram

induced a dose-dependent inhibition of GP activity with full inhibition (with 15 ± 14% of control) obtained with 20 μM.

The specific reactivity of DTCs toward cysteine residues suggest that reducing agents, including the reducing agent DTT, at least partially, restore protein functions. To investigate the reversibility of endogenous GP inhibition by thiram, we further incubated brain extracts treated with thiram and DTT. As shown in Fig. 1C, DTT partially restored endogenous GP activity (57 ± 13% of control), suggesting the formation of both reversible and irreversible modifications of GP enzymes in the brain by thiram treatment.

bGP Is Reversibly Inhibited by Thiram through the Modification of Cysteine Residues and Intramolecular Disulfide Bonds—In the brain, bGP is both expressed in astrocytes and in neurons. To investigate the molecular mechanism of GP inhibition by DTCs, we first exposed the recombinant human bGP to increasing concentrations of thiram (0.5–10 μM) (Fig. 2a). The bGP was inhibited in a dose-dependent manner with an IC₅₀ value of 1 μM, similar to what we observed with mice brain homogenates. We also investigated the impact of other DTCs on human bGP (Fig. 1A). As shown in Table 1, other DTCs such as disulfiram, as well as metal-complexed DTCs such as maneb and mancozeb, also lead to the inhibition of the recombinant enzyme (with residual activities comprised between 15 and 35% of the positive control), confirming the high sensitivity of bGP to DTCs.

To ascertain whether bGP was inhibited by thiram through the covalent modification of the enzyme, thiram-inhibited bGP was buffer-exchanged using a PD10 column. In agreement with DTC reactivity (covalent modification of cysteines) (1, 4), thiram-exposed bGP demonstrated a residual activity of 25% before and after buffer exchange, suggesting that the enzyme is covalently inhibited by thiram (Fig. 2b). In addition, we carried out second order kinetic analysis and determined the second order rate constant (k_{inact}) of bGP inhibition by thiram. We obtained a k_{inact} of $1.4 \times 10^5 \text{ M}^{-1} \text{ s}^{-1}$ (Fig. 2c), suggesting a fast inhibition of the enzyme within seconds, in agreement with previously reported for other enzymatic systems (28–30).

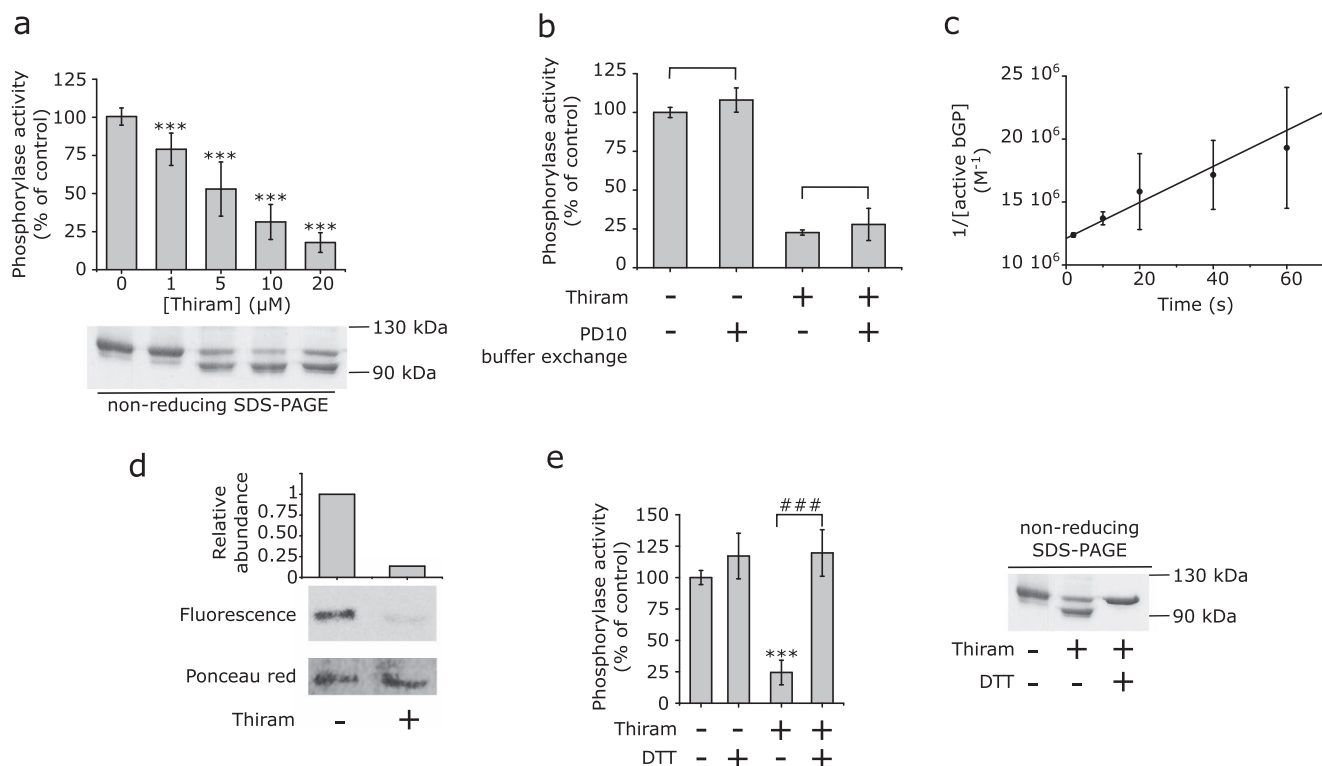


FIGURE 2. Thiram inhibits bGP through the reversible formation of intramolecular disulfide bonds. *a*, recombinant bGP was incubated with different concentrations of thiram (0–10 μM) for 30 min at 37 °C. Residual activity was assayed, and aliquots were also subjected to SDS-PAGE analysis under non-reducing conditions. The results are expressed as percentages of the control. The data represent mean values of three independent experiments ± S.D., ****p* < 0.001 compared with positive control. *b*, recombinant bGP was incubated with 10 μM thiram as previously described and was then subjected to buffer exchange using PD10 desalting column. Activity was then measured and expressed as percentages of the positive control. *c*, second order rate constant was then determined under equimolar condition by incubating 1 μM bGP with 1 μM thiram. An aliquot was removed every 10 s and assayed for residual activity. The results are expressed as 1/[active bGP] in function of time. The solid line represents the best linear regression fit of the data to Equation 1. The calculated k_{inact} for the inhibition of bGP by thiram was $1.4 \times 10^{-5} \text{ M}^{-1} \text{ min}^{-1}$. The data represent the mean values of one representative experiment ± S.D. *d*, to confirm the modification of cysteine residues upon exposure to thiram, recombinant bGP was inhibited by thiram, and free cysteine residues were specifically labeled using the fluorescent probe 5-IAF. Samples were run on SDS-PAGE in the presence of 2-mercaptoethanol and blotted onto nitrocellulose membrane. 5-IAF fluorescence was measured (λ_{exc} was 492 nm, and λ_{em} was 520 nm), and bGP was revealed by Ponceau red coloration. The untreated bGP is used as a positive control. *e*, recombinant bGP was first inhibited by thiram and subsequently incubated with 5 mM DTT prior to activity measurement and SDS-PAGE analysis.

TABLE 1
bGP inhibition by DTC

Recombinant bGP was incubated with 10 μM of DTC for 30 min at 37 °C prior to activity measurement.

Compound	Phosphorylase residual activity
	% of control ± S.D.
Control	100 ± 5.62
Thiram	21.25 ± 9.11
Disulfiram	23.94 ± 2.85
Maneb	16.26 ± 11.7
Mancozeb	34.48 ± 2.48

As we stated above, DTCs are known to interact with proteins through the formation of mixed disulfide (adducts) with cysteine residues and/or to induce the formation of disulfide bonds (1, 4) (Fig. 1*B*). 5-Iodoacetamide-fluorescein (5-IAF), an alkylating agent that specifically and covalently modifies reduced thiol groups, was used in chemical labeling experiments to investigate the modification of bGP cysteines by thiram. The results presented in Fig. 2*d* show that treatment with thiram leads to a loss of 5-IAF fluorescence signal, indicating a reduction of cysteine alkylation by 5-IAF after treatment. These results thus confirmed the modification of cysteines residues of bGP upon thiram exposure. Furthermore, SDS-PAGE of treated and untreated bGP showed that inhibited bGP migrated

faster than the positive control, indicating the formation of intramolecular disulfide bonds upon treatment with thiram (Fig. 2*a*, lower panel).

Because disulfide bonds are oxidative modifications of proteins that can be reduced by reducing agents, we carried out reactivation experiments using DTT. As shown in Fig. 2*e*, DTT fully reactivated bGP and restored the migration profile bGP on SDS-PAGE similarly to the control enzyme (non-treated bGP). Together, these findings indicated that bGP inhibition by thiram occurred through the reversible modification of cysteine residues with the concomitant formation of intramolecular disulfide bonds.

bGP Is Inhibited by Parent Thiram and Certain Oxidative Metabolites—DTCs, such as thiram, can be metabolized to different reactive metabolites that lead to the reversible and/or irreversible modification of cysteine residues (1). Indeed, DTCs such as thiram are readily reduced in blood and can undergo intracellular re-oxidation (31). In addition, they can be decomposed leading to the formation of isothiocyanate of carbon disulfide intermediates. Additionally, reduced DTCs might also be oxidized to sulfoxide and sulfone derivatives (Fig. 3*a*) (7, 24, 32, 33). Interestingly, all are able to interact with cysteine lateral side chain (albeit with different reactivities) and to impact protein functions (4, 7). We thus investigated the impact of DTC

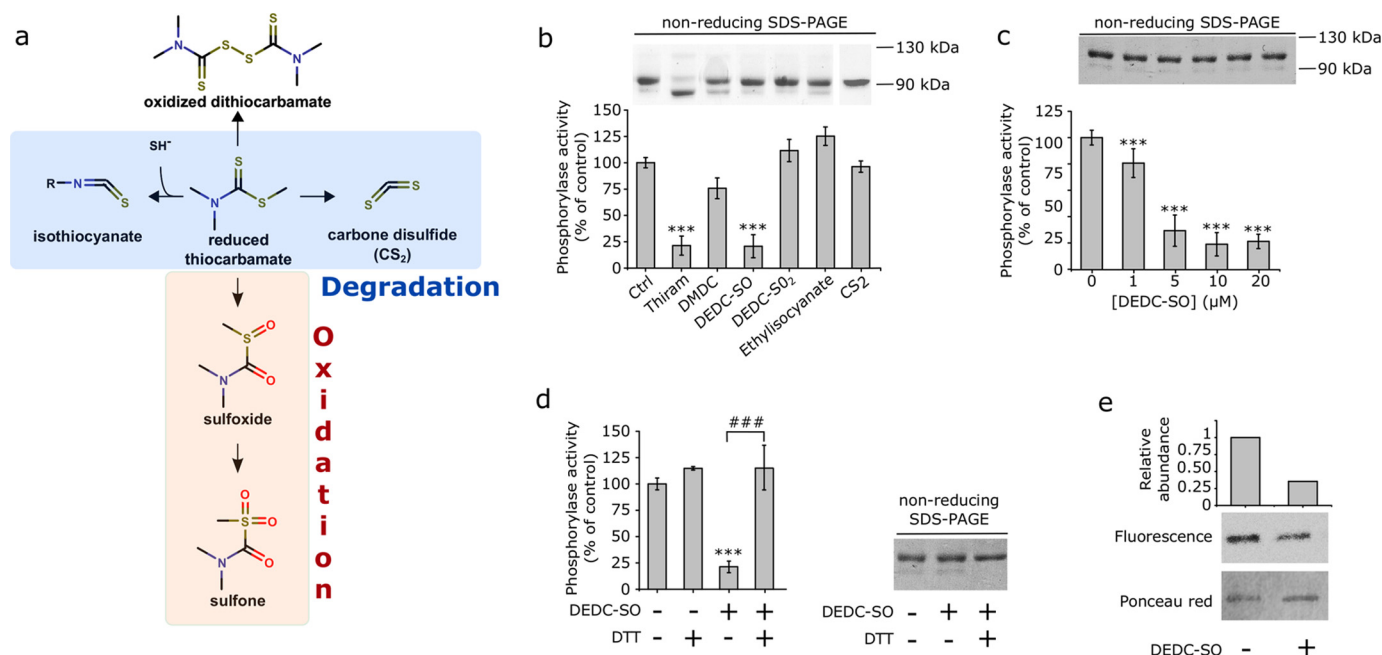


FIGURE 3. bGP is inhibited by thiram metabolites DEDC-sulfoxide. *a*, the metabolism of DTCs. In the organism, DTCs are found as an equilibrium between their reduced and oxidized form. In addition, reduced DTCs can be decomposed in carbon disulfide (CS₂) and isothiocyanate. In addition, DTCs can undergo oxidation and form sulfoxide and sulfone metabolites. *b*, recombinant bGP was independently incubated with 10 μM of thiram metabolites for 30 min at 37 °C prior to activity measurement and SDS-PAGE analysis. *c*, recombinant bGP was incubated with different concentrations of DEDC-sulfoxide (0–10 μM) for 30 min at 37 °C. Residual activity was assayed, and aliquots were also subjected to SDS-PAGE analysis under non-reducing conditions. The results are expressed as percentages of the control. The data represent mean values of three independent experiments ± S.D. ****p* < 0.001 compared with positive control. *d*, recombinant bGP was first inhibited by DEDC-sulfoxide and subsequently incubated with 5 mM DTT prior to activity measurement and SDS-PAGE analysis. *e*, to confirm the modification of cysteine residues upon exposure to DEDC-sulfoxide, recombinant bGP was inhibited by thiram, and free cysteine residues were specifically labeled using the fluorescent probe 5-IAF. The samples were run on SDS-PAGE in the presence of 2-mercaptoethanol and blotted onto nitrocellulose membrane. 5-IAF fluorescence was measured (λ_{exc} was 492 nm, and λ_{em} was 520 nm), and bGP was revealed by Ponceau red coloration. The untreated bGP is used as a positive control.

metabolites on bGP activity. Because the metabolites of thiram (DMDC-sulfoxide, DMDC-sulfone, and methylisothiocyanate) are not commercially available, we used the metabolites of disulfiram (DEDC-sulfoxide, DEDC-sulfone, and ethylisothiocyanate), which only differ from thiram metabolites by one methyl group (4, 7). As shown in Fig. 3*b*, DEDC-sulfoxide metabolite was found to be a potent inhibitor of bGP similar to what we found for thiram. However, we did not observe inhibition of bGP activity following incubation with DEDC-sulfone, isothiocyanate, or carbon disulfide (Fig. 3*b*). These results suggest that thiram but also certain metabolites might be involved in the inhibition of bGP. We further investigated the inhibition of bGP by DEDC-sulfoxide by treating the recombinant bGP with increasing concentrations of this metabolite. Similarly to what we found with thiram, bGP was inhibited in a dose-dependent manner (Fig. 3, *c* and *d*) and was concomitant with a loss of 5-IAF fluorescence signal (Fig. 3*e*), suggesting that inhibition occurred through the modification of essential sulfhydryl groups of cysteine residues. However, DEDC-sulfoxide exposure of bGP did not lead to a shift in bGP migration on SDS-PAGE (Fig. 3, *b* and *c*). Sulfoxide metabolites of DTCs are known to induce bonds (34), as well as adducts on cysteines (24). Recently, bGP has been shown to be regulated through the formation of intramolecular disulfide bonds that do not impact the migration profile of the enzyme (23). Consequently, bGP inhibition by DEDC-sulfoxide is likely to be due to either adduction of cysteine residues and/or formation of intramolecular disulfide bonds that do not impact migration profile.

Cys³¹⁸ and Cys³²⁶ Are Involved in bGP Inhibition by Thiram—bGP has 12 cysteine residues in its primary sequence. Using the crystal structure of the human bGP (35), we previously identified two potential intramolecular disulfide bonds: between Cys³¹⁸ and Cys³²⁶ and between Cys³⁷³ and Cys⁴⁴⁵ (Fig. 4, *a* and *b*), the first one being specific for the brain isoform of GP (Cys³²⁶ is not present in muscle and liver GPs) and involved in the redox regulation of bGP activity (23). To test whether this disulfide bond was involved in bGP inhibition by thiram, we performed site-directed mutagenesis experiments, substituting Cys³¹⁸ and Cys³²⁶ with serine residues, and treated the mutated enzymes with thiram. As shown in Fig. 4*c*, mutation of Cys³¹⁸ or Cys³²⁶, as well as the simultaneous mutation of the two cysteines into serine residues protected bGP from its inhibition by thiram, indicating that the modification of these cysteine residues (likely through disulfide bonds) was involved in bGP inhibition by thiram. Similar protection was observed after exposing WT and mutants bGP to DEDC-sulfoxide (Fig. 4*d*), indicating that this metabolite likely inhibits bGP through the modification of these cysteine residues and disulfide bond formation. Moreover, despite the bGP mutants being fully active following exposure to thiram, non-reducing SDS-PAGE analysis showed that the enzymes still presented a shift in their migration profile, suggesting that disulfide bonds still occurred after treatment by thiram without obvious effect on the enzyme activity (Fig. 4*c*). Because Cys³⁷³ and Cys⁴⁴⁵ can be involved in a disulfide bond as well, it is likely that this bond still forms after exposure to thiram but has no impact on the activity. The mod-

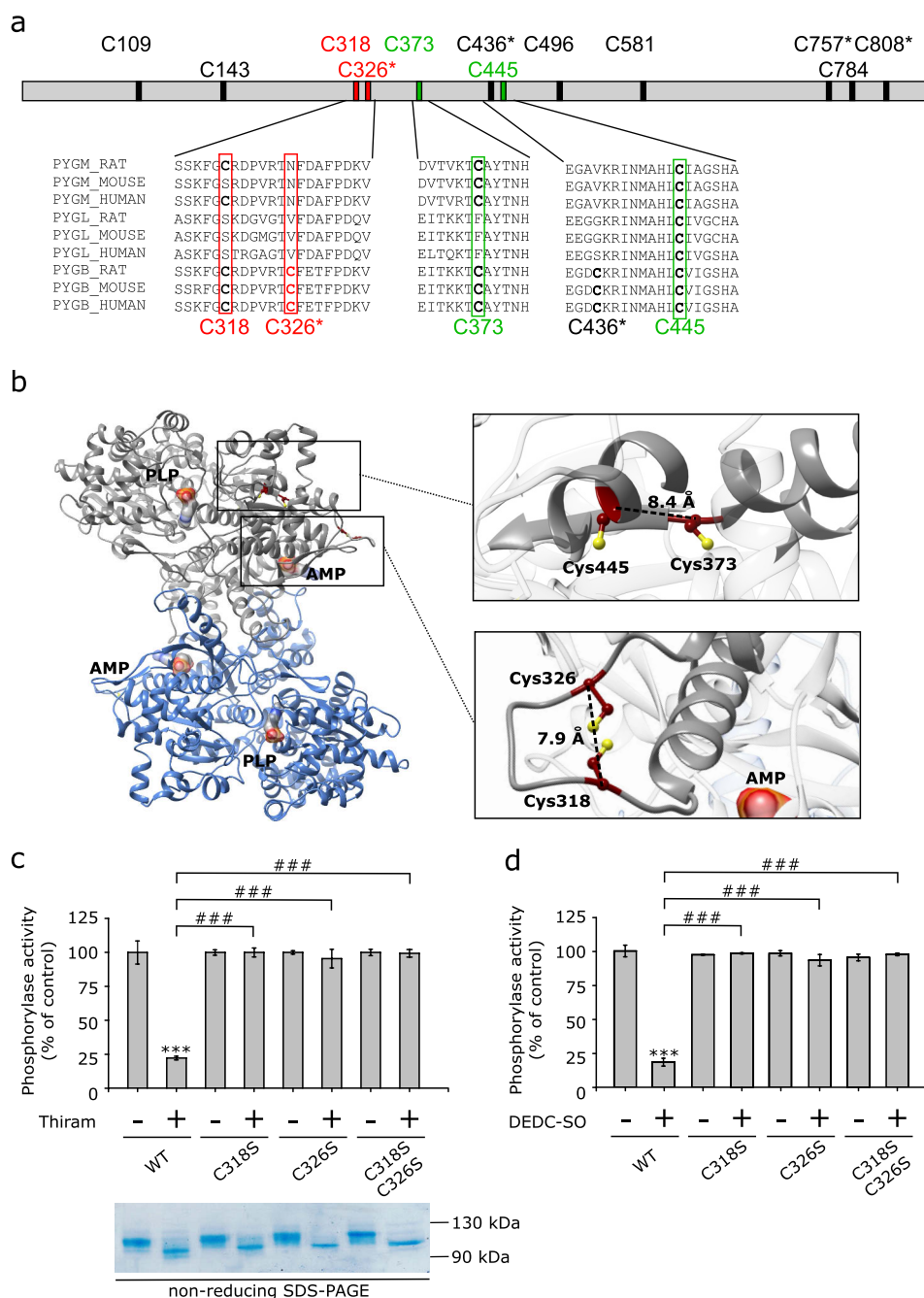


FIGURE 4. Thiram induced the formation of the Cys³¹⁸–Cys³²⁶ disulfide bond, which impairs bGP activity. *a*, bGP sequence representation with relative positions of the cysteine residues. Four cysteine residues are specific from the brain isoform (C326*, C436*, C757*, and C808*). Cys³¹⁸ and Cys³²⁶, which have been previously identified as forming an intramolecular disulfide bond are presented in red. Cys³⁷³ and Cys⁴⁴⁵, which can also form an intramolecular disulfide bond are presented in green. Sequences of muscle (PYGM), liver (PYGL), and brain (PYGB) glycogen phosphorylase from rat, mouse, and human containing these four cysteines have been aligned. *b*, ribbon representation of α trace of the dimer of bGP. The AMP-binding site is marked by the allosteric effector AMP (surface representation). Cys³¹⁸, Cys³²⁶, Cys³⁷³, and Cys⁴⁴⁵ are represented as red sticks and balls. The distance separating the α of Cys³¹⁸ and Cys³²⁶ (7.9 Å), as well as Cys³⁷³ and Cys⁴⁴⁵ (8.4 Å) is shown. *c*, single mutation and double mutations of Cys³¹⁸ and Cys³²⁶ were performed and tested for thiram inhibition resistance as described above. The results are expressed as percentages of the control. The data represent the mean values of three independent experiments \pm S.D. ***, $p < 0.001$ compared with control. *d*, to determine whether Cys³¹⁸ and Cys³²⁶ are involved in the inhibition of bGP by DEDC-sulfoxide, WT, and mutants (C318S, C326S, C318S/C326S) were incubated with DEDC-sulfoxide for 30 min at 37 °C prior to activity measurement. The data represent mean values of three independent experiments \pm S.D. ***, $p < 0.001$ compared with positive control.

ification of Cys³¹⁸, Cys³²⁶, Cys³⁷³, and Cys⁴⁴⁵ was confirmed by differential labeling of cysteine residues and LC-MS/MS analysis, following treatment by thiram (supplemental Fig. S1).

AMP-dependent Activation of bGP Is Altered by Thiram but Not Phosphorylation-dependent Activation of bGP—GPs are allosteric enzymes found in at least two states: an inactive state

(or T-state) and an active state (or R-state). GP activation is under the control of the binding of AMP in the AMP binding site and/or the phosphorylation of Ser¹⁴. Cys³¹⁸ and Cys³²⁶ are located in the adenine loop of bGP, which belongs to the AMP binding site. We previously reported that the formation of an intramolecular disulfide bond between Cys³¹⁸ and Cys³²⁶ by

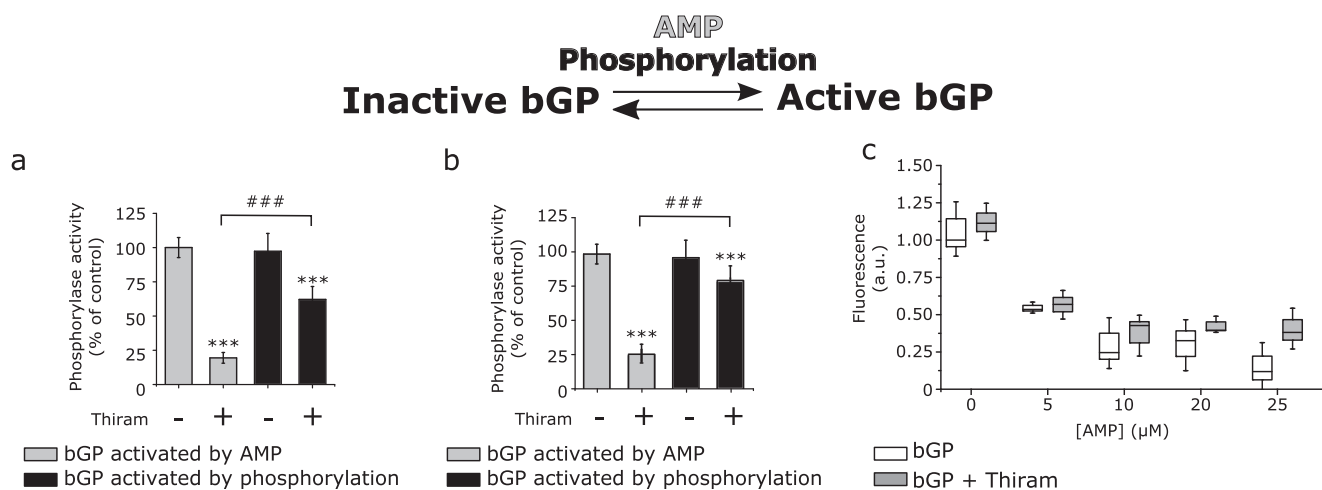


FIGURE 5. Thiram induced Cys³¹⁸/Cys³²⁶ disulfide bond alter the AMP-dependent regulation of bGP by blocking the transmission of the allosteric signal. *a*, bGP was incubated with 10 μ M thiram for 30 min at 37 °C. The inhibited enzyme was then incubated with AMP or phosphorylase kinase prior to activity measurement. The results are expressed as percentages of the control. The data represent mean values of three independent experiments \pm S.D. ***, $p < 0.001$ compared with control; ###, $p < 0.001$ when two groups are compared. *b*, to assess the inhibition of active R state bGP by thiram, bGP was preincubated with AMP or phosphorylase kinase prior to exposure to 10 μ M thiram. The mixture was then assayed for activity measurement. The results are expressed as percentages of the control. The data represent mean values of three independent experiments \pm S.D. ***, $p < 0.001$ compared with control; ###, $p < 0.001$ when two groups are compared. *c*, analysis of the binding of AMP to reduced and oxidized bGP was performed by incubating the treated or untreated enzyme with 5 μ M of fluorescent mant-AMP. To ascertain that the fluorescence was due to binding of mant-AMP to the enzyme, increasing concentrations of AMP were added. The addition of increasing concentration of AMP resulted in a loss of fluorescence.

H₂O₂ can alter bGP activation by its allosteric activator AMP without affecting its activation by phosphorylation (23). To determine the impact of thiram on the allosteric regulation of bGP, we first determined whether AMP or phosphorylation were able to activate bGP following thiram exposure. As shown in Fig. 5*a*, AMP did not activate the thiram-treated enzyme, whereas the phosphorylation of thiram-treated bGP significantly triggered its activation (Fig. 5*a*). In the next set of experiments, we further investigated the impact of thiram on bGP activation using the activated (R state) enzyme. To this end AMP-activated bGP or phosphorylated bGP were treated with thiram prior to activity measurement. We observed that the phosphorylated enzyme remained active, whereas the AMP-activated enzyme was inhibited by thiram (Fig. 5*b*). Together, these results suggested that thiram poorly affects the phosphorylation-dependent activation of bGP but alters the AMP-dependent activation of the enzyme.

Finally, we used the fluorescent AMP analog mant-AMP to investigate the ability of the treated enzyme to bind AMP. When it binds to proteins, mant-AMP emits a fluorescence signal that decreases following the addition of AMP (Fig. 5*c*). We found similar behavior in the treated and non-treated enzymes toward mant-AMP binding, suggesting that the thiram-induced Cys³¹⁸–Cys³²⁶ disulfide bond did not modify the binding of AMP in the AMP binding site but likely altered the transmission of the allosteric activation signal (Fig. 5*c*).

Discussion

DTCs are highly reactive compounds widely used as pesticides, in the industry and in several therapeutic applications (1). These chemicals are highly reactive and covalently modify proteins through the adduction of cysteine residues and/or the subsequent formation of disulfide bonds (1, 4). The wide use of DTCs has raised many concerns about their impact on the environment and human health. Many studies have thus associated

DTCs with the development of several pathologies including the Parkinson's disease-like syndromes (2, 3). However, the molecular basis of DTC toxicity in the brain is poorly understood. Here, we report that bGP activity is impaired by DTCs such as thiram, as well as certain DTC oxidative metabolites. Using human recombinant bGP enzyme, we demonstrated that thiram and certain metabolites (sulfoxide form) inhibited bGP activity through the modification of cysteine residues and the subsequent formation of intramolecular disulfide bonds (Figs. 1*B* and 2). One of the disulfide bonds involved Cys³¹⁸ and Cys³²⁶, two cysteines located in the AMP binding site that participated to the activation of bGP by the allosteric activator AMP (Fig. 4) (23). GPs are allosteric enzymes tightly regulated by the binding of allosteric effectors, including AMP, and by phosphorylation, in response to extracellular signals (such as neurotransmitters). We found that thiram induces the formation of a disulfide bond between Cys³¹⁸ and Cys³²⁶, impairing the AMP-dependent activation but poorly affecting the phosphorylation-dependent activation of the enzyme (Fig. 5). These results suggest that DTCs and certain DTC metabolites are able to alter the activity of bGP and with possible subsequent alteration of glycogen metabolism.

Contrary to H₂O₂ oxidation, which induced the formation of the Cys³¹⁸–Cys³²⁶ disulfide bond and altered the binding of AMP in the AMP binding site, thiram-induced Cys³¹⁸–Cys³²⁶ disulfide bond did not lead to an altered binding of AMP (Fig. 5), suggesting that thiram-dependent modification of the cysteines only impairs the transmission of allosteric signal (23). In addition, the mutation of these cysteine residues fully protected the enzyme from the inhibition by thiram and metabolites, suggesting that only these two cysteines were involved in bGP inhibition by thiram. The different mechanism of inhibition of bGP (altered AMP binding and/or alteration of transmission of allosteric signal) between H₂O₂ and thiram might be associated with

the different reactivity of these chemicals. Indeed, thiram is highly reactive and can form adduct on cysteine residues (1, 4). In addition, contrary to H_2O_2 , we observed that bGP exposure to thiram also leads to the formation of a second intramolecular disulfide bond between Cys³⁷³ and Cys⁴⁴⁵. These two cysteine residues, found in the three GP isozymes, are located next to the glycogen storage site of GP, a site involved in the binding of glycogen. Although this disulfide bond does not impact bGP activation and activity (Fig. 4), it might affect the enzyme behavior toward its substrate, such as substrate affinity. Moreover, because of the conservation of these two residues among GP isoenzymes, the Cys³⁷³–Cys⁴⁴⁵ disulfide bond might also impact glycogenolysis in muscle and liver. Further studies are needed to ascertain this point.

Proteomic studies revealed highly reactive cysteine residues in bGP (Cys¹⁰⁹, Cys³²⁶, and Cys⁴⁹⁶) (25–27), which can constitute potent targets of electrophilic compounds such as DTCs. Consequently, DTCs may directly modulate glycogenolysis through the modification of key cysteine residues of bGP, known to redox regulate the enzyme activity. Moreover, considering that DTCs induce oxidative stress in cells, particularly through the depletion of the GSH pool and the inhibition of antioxidant enzymes (36–38), bGP may also constitute an indirect target a DTC through the oxidation of highly reactive cysteine residues. GP inhibition in brain extracts was not fully rescued by the subsequent addition of high concentrations of reducing agents (DTT) (Fig. 1C). It is thus likely that thiram (and other DTCs) may be metabolized to reactive metabolites (or may induce strong oxidative stress), leading to the irreversible inhibition of brain GP enzymes and subsequent alteration of glycogen metabolism. In addition, the brain displays a limited content in reducing power, which could thus emphasize the inhibition of glycogenolysis in the brain and the toxicity of DTCs (39).

The relationship between brain glycogen accumulation, and brain disease is now well established. Accumulation of glycogen in neurons is a direct cause of neurodegeneration (21) and is observed in several brain diseases, including Lafora disease, Alzheimer's disease, and amyotrophic lateral sclerosis, and in aging (21, 40–42). DTCs are known to induce several neurological effects including ataxia, convulsion, behavioral abnormalities (43), and Parkinson's disease-like syndrome (2, 3). Our results suggest that brain glycogen metabolism could be involved in the brain toxicity of DTCs, particularly through the impairment of brain energy metabolism and the toxic accumulation of glycogen in neurons and in astrocytes. In addition, the isozyme-specific inhibition of bGP by thiram suggests that DTCs constitute a basis for the development of drugs targeting glycogen metabolism.

Experimental Procedures

Materials

Thiram, Disulfiram, Maneb, Mancozeb, DMDC, isothiocyanate, carbon disulfide, protease mixture inhibitors, rabbit muscle phosphorylase kinase, phosphoglucomutase, AMP, ATP, glycogen, glucose-1,6-diphosphate, DTT, 5-IAF, and BSA were purchased from Sigma-Aldrich. Anti-bGP antibody was provided by Santa Cruz (sc-81751). DEDC-sulfoxide and DEDC-

sulfone were provided by Toronto Research Chemical Inc. Glucose-6-phosphate dehydrogenase was purchased from Roche. Mant-AMP was purchased from Jena Bioscience. NADP^+ was purchased from Apollo Scientific.

Methods

Cloning and Site-directed Mutagenesis—The human bGP cDNA was obtained in the eukaryotic pCMV6-XL4 vector (provided by OriGene Technologies, Inc.) and subcloned into the pET28a vector for expression and purification of recombinant bGPs. The resulting construct encoded for His₆-tagged fusion recombinant proteins (His-bGP). *Escherichia coli* C41(DE3)/pGro7 (encoding the GroEL/GroES chaperonin protein complex) strains were transformed with plasmid pET28a carrying His-bGP and used to express and purify the recombinant enzymes.

For site-directed mutagenesis of bGP, cysteine residues 318 and 326 were mutated into serine residues using the Agilent QuikChange site-directed mutagenesis kit according to the manufacturer's instructions. Briefly, the mutagenesis of each cysteine residue was performed by amplification of the whole plasmids (pCMV6 and pET28a) carrying bGP, using 5' and 3' primers containing the single point mutation to induce. The sequence of each oligonucleotides pair used is presented in [supplemental Table S2](#).

Expression and Purification of Recombinant bGP—Recombinant human bGP was expressed using C41 *E. coli* bacteria containing pGro7 plasmid responsible for the expression of the chaperonin protein complex GroEL/GroES and cultured at 37 °C. Expression of the GroEL/GroES chaperonin protein complex was first induced by the addition of 1 mM L-arabinose to culture. Expression of recombinant His-bGP was then induced by the addition of 500 μM of isopropyl-1-thio- β -D-galactopyranoside to culture. The bacteria were further cultured at 16 °C overnight. The bacteria were then pelleted by centrifugation ($4,000 \times g$, 10 min), washed with cold PBS, harvested by centrifugation ($4,000 \times g$, 10 min), and stored at -80 °C until required.

The bacteria were suspended in 35 ml of lysis buffer (PBS, pH 8, 300 mM NaCl, 0.5% Triton X-100, 1 mg/ml lysozyme, protease inhibitor mixture) and incubated for 1 h at 4 °C. The lysate was sonicated on ice (8-s pulses for up to 7 min) and centrifuged ($17,000 \times g$, 30 min, 4 °C). The supernatant was collected and incubated with 1 ml of nickel-nitrilotriacetic acid Superflow resin in the presence of 10 mM imidazole (final concentration) for 2 h at 4 °C. The resin was then poured into a column and washed successively with washing buffer (PBS, pH 8, 300 mM NaCl) containing 0.1% Triton X-100 and a stepwise gradient of imidazole in washing buffer until a concentration of 20 mM imidazole (final concentration) was achieved. His-tagged proteins were eluted with washing buffer containing 300 mM imidazole. Purified proteins were incubated for 10 min with 10 mM DTT and protease inhibitor mixture and then exchanged against PBS, pH 7.1, using a PD 10 desalting column. The protein concentration was measured using the standard Bradford assay with BSA as standard and by absorbance measurement at 280 nm, using a theoretical ϵ_{M} : 115,170 $\text{M}^{-1} \text{cm}^{-1}$. The purity of the protein was assessed by SDS-PAGE analysis.

GP Activity Assay—GP activity was measured in the direction of glycogen breakdown as previously described (44). Briefly, the formation of glucose-1-phosphate was determined using a coupled assay system composed of phosphoglucomutase, glucose-6-phosphate dehydrogenase and NADP, by measuring (NADPH·H⁺) formation at 340 nm. The phosphorylase activity assay was carried out at 37 °C in PBS, pH 6.9. The mixture consisted of GP (final concentration, 0.1 μM) with or without 1 mM AMP, 0.25% glycogen, 2 mM EDTA, 0.8 mM NADP, 10 mM magnesium acetate, 5 μM glucose-1,6-diphosphate, 5 units of glucose-6-phosphate dehydrogenase, and 5 units of phosphoglucomutase in a final volume of 250 μl. Each measurement was performed in triplicate. GP activity was expressed as the percentage of the control.

SDS-PAGE and Western Blotting—Proteins were loaded onto 7.5% polyacrylamide gels, and electrophoretic protein separation was carried out at 110 V (constant voltage) under non-reducing conditions. For SDS-PAGE, the presence of protein was revealed using R-250 Coomassie Blue. After SDS-PAGE, the proteins were transferred onto a nitrocellulose membrane at a constant current of 200 mA at 4 °C for 1 h. Membranes were incubated at 4 °C overnight with appropriately diluted primary antibody. After washing, the membranes were incubated for 2 h at room temperature with peroxidase-coupled secondary antibody. The proteins were visualized by chemiluminescence detection using ECL substrate and LAS 4000 (Fujifilm). The images were analyzed using Gimp 2 software.

Phosphorylation of Ser¹⁴ of bGP—bGP was phosphorylated using phosphorylase kinase from rabbit muscle (1 unit/mg bGP), activated by preincubation for 1 h in phosphorylation buffer 20 mM Tris-HCl buffer, pH 7.7, 0.22 mM ATP, 3.3 mM MgCl₂, 0.5 mM CaCl₂, 0.5 mM NaF for activation. Phosphorylation was performed by the addition of activated phosphorylase kinase to the bGP solution, in phosphorylation buffer, and incubation for 2 h at room temperature. The resulting activity was assessed with or without AMP. Phosphorylation of rabbit muscle GP was used as a control. Phosphorylated bGP was then subjected to buffer exchange against PBS buffer, pH 6.9, using a PD Minitrapp G25 (GE Healthcare) desalting column.

Effect of DTCs on Recombinant bGP Activity—To test the effect of DTCs (thiram, DMDC, disulfiram, maneb, and mancozeb) and metabolites (DEDC-sulfoxide, DEDC-sulfone, isothiocyanate, and carbon disulfide) on recombinant bGP, 1 μM recombinant human bGP was incubated with DTCs or DTC metabolites for 30 min at 37 °C in a final volume of 25 μl. The reaction was stopped by the addition of the activity assay mixture (which results in a 10 times dilution). GP activity in absence of DTCs was considered as 100% activity. Each measurement was performed in triplicate.

To determine whether thiram-dependent inhibition of bGP is irreversible, bGP exposed to thiram was exchanged against PBS, pH 7.1, using PD 10 desalting column (GE Healthcare) prior to activity assay. To test whether the reducing agent could reactivate the enzyme, recombinant bGP treated with thiram was incubated with 5 mM DTT for 10 min at 37 °C prior to activity measurement. The results are expressed as percentages of the control (enzyme in absence of thiram).

5-IAF Labeling—To test whether thiram or DEDC-sulfoxide-dependent inhibition was concomitant with the modification of cysteine residues, we performed cysteine labeling experiments using 5-IAF. To this end, 1 μM bGP was incubated with thiram as described above. The mixture was then incubated with 20 μM 5-IAF for 10 min at 37 °C and then run on SDS-PAGE under reducing condition. The proteins were then transferred on nitrocellulose membrane, and fluorescence was measured (λ_{exc} was 492 nm, and λ_{em} was 520 nm) using the ImageQuant LAS-4000 system (Fujifilm-GE Healthcare). bGP was also revealed using Ponceau red staining.

Kinetic Analysis: Determination of the Second Order Rate Constant of bGP Inhibition by Thiram—Second order rate constant of inhibition of bGP by thiram was obtained under second order conditions (equal concentration of bGP and thiram). 1 μM bGP was incubated with 1 μM thiram at 37 °C. Aliquots of the mixture were taken every 10 s, and the reaction was stopped by the addition of the activity assay mixture. The *k*_{inact} value was obtained by fitting the data to the following equation,

$$1/E = 1/E_0 + k_{\text{inact}} \times t \quad (\text{Eq. 1})$$

where *E* is the concentration of active bGP at time *t*, and *E*₀ is the initial concentration of active bGP. Kinetic data were analyzed using Origin Pro 8 software and a *k*_{inact} value of 1.4 10⁵ M^{−1} s^{−1} was obtained.

Mass Spectrometry Analysis—bGP was fully reduced and precipitated using TCA to stabilize cysteine residues. Proteins were then centrifuged, and pellets were successively washed using 1) acetone containing 5 mM HCl and 2) acetone. We employed mass spectrometry with differential cysteine labeling to identify the modified cysteines in the enzyme. With that aim, 1 μM of precipitated bGP was resuspended in PBS buffer containing 250 mM IAA or incubated with 2 mM thiram for 10 min at room temperature. Proteins were precipitated again using TCA and washed as previously described. Pellets were finally resuspended in loading buffer containing 250 mM IAA to alkylate any unreacted cysteine residues. The samples were first purified on a 7.5% SDS-polyacrylamide gel stained with Coomassie blue R250. After in-gel reduction (final concentration, 5 mM DTT; 30 min, 56 °C) and alkylation (200 mM NEM for 20 min at room temperature in the dark), gels slices are recovered by trypsin (Roche) at 12.5 ng/μl in 25 mM ammonium bicarbonate, 0.05% CaCl₂ and incubated overnight at 37 °C. Then the reaction was stopped with 100 μl of 5% formic acid. Peptides were extracted from gel and incubated twice in 5% formic acid prior to sonication and incubation acetonitrile. Then supernatants from all the fractions of the same sample were pooled and dried using a SpeedVac.

Samples were purified by Zip-Tip (Millipore) before the LC-MS/MS analysis by eluting in a solution containing 60% acetonitrile, 0.1% formic acid. Desalted samples were then diluted 10 times prior to fractionation on a capillary reverse phase column (nano C18 Dionex Acclaim PepMap100, 75 μm inner diameter × 50 cm) at constant flow rate of 220 nl/min, with a gradient of 2% to 40% of buffer B containing 90% acetonitrile, 10% water, 0.1% formic acid (buffer A: 98% water, 2% acetonitrile, 0.1% formic acid). LC was directly coupled to a Qq Orbitrap mass

spectrometer (Q Exactive, ThermoFisher Scientific). MS experiments consisted of a survey MS scan (400–2,000 m/z ; resolution 70,000) followed by an MS/MS analysis of the most 10 intense precursors, with a dynamic exclusion of 30 s of the previously fragmented precursors.

After processing raw files with the in house-developed software MaxQuant 1.5.3.8, (45) data were searched against the PYGB sequence with Andromeda (46). Carbamidomethylated cysteines and NEM cysteines were set as variable as modification like oxidation of methionine, and N-terminal acetylation. Mass deviation of 0.5 D was set as maximum allowed for MS/MS peaks, and a maximum of two missed cleavages were allowed. Maximum false discovery rates were set to 0.01 both on peptide and protein levels. The minimum required peptide length was 7 amino acids.

Perseus v.1.5.1.6 was used for data analysis and processing. We use the evidence.txt file to compare the abundance for each peptide modified with carbamidomethyl (CAM) or NEM. The results are expressed as the ratios of NEM/CAM labeling. A decrease in the NEM/CAM ratio suggests that the cysteine residue is modified upon addition of thiram.

AMP Binding—AMP binding experiments were carried out using fluorescent mant-AMP, an analog of AMP that fluoresces when bound to proteins. bGP (0.25 μM , either reduced or treated) was incubated with mant-AMP (5 μM) and increasing concentrations of AMP (0–50 μM) in Tris-HCl buffer, pH 7.5, for 30 min at 25 °C. Fluorescence of bound mant-AMP was determined by spectrofluorometry using $\lambda_{\text{exc}} = 355 \text{ nm}$, $\lambda_{\text{em}} = 448 \text{ nm}$ (Flex Station 3; Molecular Devices).

Total Brain Extraction and Exposure to DTCs—Three-month-old male Swiss mice brains were crushed in PBS buffer, pH 7.1 0.5% Triton, protease inhibitors mixture prior to short sonication pulses. The samples were then centrifuged during 30 min at 15,000 $\times g$, and the protein concentration was determined using the standard Bradford assay with BSA as standard. 0.125 mg/ml of brain extract were then exposed to the indicated concentrations of thiram for 30 min at 37 °C prior to activity measurement, as described above. Reactivation of GP activity by reducing agents was investigated by further incubating the sample with 10 mM DTT for 10 min at 37 °C, prior to activity assay.

Statistical Analysis—The results are presented as means \pm S.D. of three independent experiments. Statistical analysis was performed using one-way analysis of variance followed by Bonferroni's post hoc test, using OriginPro 8 software. If only two groups were compared, a mean comparison t test was used. A $p < 0.05$ was considered to be significant. $p < 0.05$, $p < 0.01$, and $p < 0.001$ are indicated by one, two, and three asterisks.

Author Contributions—C. M., F. R.-L. designed experiments, managed the project, and wrote the manuscript. C. M., L.-C. B., E. P., I. H., O. A., J. V., J.-M. D., and F. R.-L. contributed reagents, performed experiments, and/or analyzed the data. All the authors discussed the results and commented on the manuscript.

References

- Mathieu, C., Duval, R., Xu, X., Rodrigues-Lima, F., and Dupret, J.-M. (2015) Effects of pesticide chemicals on the activity of metabolic enzymes: focus on thiocarbamates. *Expert Opin. Drug Metab. Toxicol.* **11**, 81–94
- Wang, A., Costello, S., Cockburn, M., Zhang, X., Bronstein, J., and Ritz, B. (2011) Parkinson's disease risk from ambient exposure to pesticides. *Eur. J. Epidemiol.* **26**, 547–555
- Brown, T. P., Rumsby, P. C., Capleton, A. C., Rushton, L., and Levy, L. S. (2006) Pesticides and Parkinson's disease: is there a link? *Environ. Health Perspect.* **114**, 156–164
- Shen, M. L., Lipsky, J. J., and Naylor, S. (2000) Role of disulfiram in the *in vitro* inhibition of rat liver mitochondrial aldehyde dehydrogenase. *Biochem. Pharmacol.* **60**, 947–953
- Ferraz, H. B., Bertolucci, P. H., Pereira, J. S., Lima, J. G., and Andrade, L. A. (1988) Chronic exposure to the fungicide maneb may produce symptoms and signs of CNS manganese intoxication. *Neurology* **38**, 550–553
- Meco, G., Bonifati, V., Vanacore, N., and Fabrizio, E. (1994) Parkinsonism after chronic exposure to the fungicide maneb (manganese ethylene-bis-dithiocarbamate). *Scand. J. Work. Environ. Health* **20**, 301–305
- Viquez, O. M., Caito, S. W., McDonald, W. H., Friedman, D. B., and Valentine, W. M. (2012) Electrophilic adduction of ubiquitin activating enzyme E1 by *N,N*-diethyldithiocarbamate inhibits ubiquitin activation and is accompanied by striatal injury in the rat. *Chem. Res. Toxicol.* **25**, 2310–2321
- Sook Han, M., Shin, K. J., Kim, Y. H., Kim, S. H., Lee, T., Kim, E., Ho Ryu, S., and Suh, P. G. (2003) Thiram and ziram stimulate non-selective cation channel and induce apoptosis in PC12 cells. *Neurotoxicology* **24**, 425–434
- Vaccari, A., Saba, P., Mocci, L., and Rui, S. (1999) Dithiocarbamate pesticides affect glutamate transport in brain synaptic vesicles. *J. Pharmacol. Exp. Ther.* **288**, 1–5
- Rahman, M. A., Grunberg, N. E., and Mueller, G. P. (1997) Disulfiram causes sustained behavioral and biochemical effects in rats. *Pharmacol. Biochem. Behav.* **56**, 409–415
- Kona, F. R., Buac, D., and Burger, M. A. (2011) Disulfiram, and disulfiram derivatives as novel potential anticancer drugs targeting the ubiquitin-proteasome system in both preclinical and clinical studies. *Curr. Cancer Drug Targets.* **11**, 338–346
- Amici, M., Forti, K., Nobili, C., Lupidi, G., Angeletti, M., Fioretti, E., and Eleuteri, A. M. (2002) Effect of neurotoxic metal ions on the proteolytic activities of the 20S proteasome from bovine brain. *J. Biol. Inorg. Chem.* **7**, 750–756
- Cataldo, A. M., and Broadwell, R. D. (1986) Cytochemical identification of cerebral glycogen and glucose-6-phosphatase activity under normal and experimental conditions. II. Choroid plexus and ependymal epithelia, endothelia and pericytes. *J. Neurocytol.* **15**, 511–524
- Pfeiffer-Guglielmi, B., Fleckenstein, B., Jung, G., and Hamprecht, B. (2003) Immunocytochemical localization of glycogen phosphorylase isozymes in rat nervous tissues by using isozyme-specific antibodies. *J. Neurochem.* **85**, 73–81
- Saez, I., Duran, J., Sinadinos, C., Beltran, A., Yanes, O., Tevy, M. F., Martínez-Pons, C., Milán, M., and Guinovart, J. J. (2014) Neurons have an active glycogen metabolism that contributes to tolerance to hypoxia. *J. Cereb. Blood Flow Metab.* **34**, 945–955
- Sickmann, H. M., Waagepetersen, H. S., Schousboe, A., Benie, A. J., and Bouman, S. D. (2012) Brain glycogen and its role in supporting glutamate and GABA homeostasis in a type 2 diabetes rat model. *Neurochem. Int.* **60**, 267–275
- Suzuki, A., Stern, S. A., Bozdagi, O., Huntley, G. W., Walker, R. H., Magistretti, P. J., and Alberini, C. M. (2011) Astrocyte-neuron lactate transport is required for long-term memory formation. *Cell* **144**, 810–823
- Gibbs, M. E. (2015) Role of glycogenolysis in memory and learning: regulation by noradrenaline, serotonin and ATP. *Front. Integr. Neurosci.* **9**, 70
- Suh, S. W., Bergher, J. P., Anderson, C. M., Treadway, J. L., Fosgerau, K., and Swanson, R. A. (2007) Astrocyte glycogen sustains neuronal activity during hypoglycemia: studies with the glycogen phosphorylase inhibitor CP-316,819 ([*R**,*S**]-5-chloro-*N*-[2-hydroxy-3-(methoxymethylamino)-3-oxo-1-(phenylmethyl)propyl]-1H-indole-2-carboxamide). *J. Pharmacol. Exp. Ther.* **321**, 45–50
- Choi, I.-Y., Seaquist, E. R., and Gruetter, R. (2003) Effect of hypoglycemia on brain glycogen metabolism *in vivo*. *J. Neurosci. Res.* **72**, 25–32
- Duran, J., Gruart, A., García-Rocha, M., Delgado-García, J. M., and Guinovart, J. J. (2014) Glycogen accumulation underlies neurodegeneration

- and autophagy impairment in Lafora disease. *Hum. Mol. Genet.* **23**, 3147–3156
22. Roach, P. J. (2002) Glycogen and its metabolism. *Curr. Mol. Med.* **2**, 101–120
23. Mathieu, C., Duval, R., Coccagn, A., Petit, E., Bui, L.-C., Haddad, I., Vinh, J., Etchebest, C., Dupret, J.-M., and Rodrigues-Lima, F. (2016) An isozyme-specific redox switch in human brain glycogen phosphorylase modulates its allosteric activation by AMP. *J. Biol. Chem.* **291**, 23842–23853
24. Veverka, K. A., Johnson, K. L., Mays, D. C., Lipsky, J. J., and Naylor, S. (1997) Inhibition of aldehyde dehydrogenase by disulfiram and its metabolite methyl diethylthiocarbamoyl-sulfoxide. *Biochem. Pharmacol.* **53**, 511–518
25. Weerapana, E., Wang, C., Simon, G. M., Richter, F., Khare, S., Dillon, M. B., Bachovchin, D. A., Mowen, K., Baker, D., and Cravatt, B. F. (2010) Quantitative reactivity profiling predicts functional cysteines in proteomes. *Nature* **468**, 790–795
26. Wang, C., Weerapana, E., Blewett, M. M., and Cravatt, B. F. (2014) A chemoproteomic platform to quantitatively map targets of lipid-derived electrophiles. *Nat. Methods* **11**, 79–85
27. Gould, N. S., Evans, P., Martínez-Acedo, P., Marino, S. M., Gladyshev, V. N., Carroll, K. S., and Ischiropoulos, H. (2015) Site-specific proteomic mapping identifies selectively modified regulatory cysteine residues in functionally distinct protein networks. *Chem. Biol.* **22**, 965–975
28. Nobel, C. S., Kimland, M., Nicholson, D. W., Orrenius, S., and Slater, A. F. (1997) Disulfiram is a potent inhibitor of proteases of the caspase family. *Chem. Res. Toxicol.* **10**, 1319–1324
29. Malka, F., Dairou, J., Ragunathan, N., Dupret, J.-M., and Rodrigues-Lima, F. (2009) Mechanisms and kinetics of human arylamine *N*-acetyltransferase 1 inhibition by disulfiram. *FEBS J.* **276**, 4900–4908
30. Pratt-Hyatt, M., Lin, H. L., and Hollenberg, P. F. (2010) Mechanism-based inactivation of human CYP2E1 by diethyldithiocarbamate. *Drug Metab. Dispos.* **38**, 2286–2292
31. Stromme, J. H. (1963) Effects of diethyldithiocarbamate and disulfiram on glucose metabolism and glutathione content of human erythrocytes. *Biochem. Pharmacol.* **12**, 705–715
32. Madan, A., Parkinson, A., and Faiman, M. D. (1998) Identification of the human P-450 enzymes responsible for the sulfoxidation and thiono-oxidation of diethyldithiocarbamate methyl ester: role of P-450 enzymes in disulfiram bioactivation. *Alcohol. Clin. Exp. Res.* **22**, 1212–1219
33. Madan, A., Parkinson, A., and Faiman, M. D. (1995) Identification of the human and rat P450 enzymes responsible for the sulfoxidation of *S*-methyl *N,N*-diethylthiolcarbamate (DETC-ME). The terminal step in the bioactivation of disulfiram. *Drug Metab. Dispos.* **23**, 1153–1162
34. Tam, J. P., Wu, C. R., Liu, W., and Zhang, J. W. (1991) Disulfide bond formation in peptides by dimethyl sulfoxide: scope and applications. *J. Am. Chem. Soc.* **113**, 6657–6662
35. Mathieu, C., de la Sierra-Gallay, I. L., Duval, R., Xu, X., Coccagn, A., Léger, T., Woffendin, G., Camadro, J.-M., Etchebest, C., Haouz, A., Dupret, J.-M., and Rodrigues-Lima, F. (2016) Insights into brain glycogen metabolism: the structure of human brain glycogen phosphorylase. *J. Biol. Chem.* **291**, 18072–18083
36. Biswas, S. K., and Rahman, I. (2009) Environmental toxicity, redox signaling and lung inflammation: the role of glutathione. *Mol. Aspects Med.* **30**, 60–76
37. Iqbal, J., and Whitney, P. (1991) Use of cyanide and diethyldithiocarbamate in the assay of superoxide dismutases. *Free Radic. Biol. Med.* **10**, 69–77
38. Domico, L. M., Cooper, K. R., Bernard, L. P., and Zeevalk, G. D. (2007) Reactive oxygen species generation by the ethylene-bis-dithiocarbamate (EBDC) fungicide mancozeb and its contribution to neuronal toxicity in mesencephalic cells. *Neurotoxicology* **28**, 1079–1091
39. de la Cruz, V. P., Korrapati, S. V., and Chaverri, J. P. (2015) Redox status and aging link in neurodegenerative diseases 2015. *Oxid. Med. Cell Longev.* **2015**, 494316
40. Gertz, H. J., Cervos-Navarro, J., Frydl, V., and Schultz, F. (1985) Glycogen accumulation of the aging human brain. *Mech. Ageing Dev.* **31**, 25–35
41. Dodge, J. C., Treleaven, C. M., Fidler, J. A., Tamsett, T. J., Bao, C., Searles, M., Taksir, T. V., Misra, K., Sidman, R. L., Cheng, S. H., and Shihabuddin, L. S. (2013) Metabolic signatures of amyotrophic lateral sclerosis reveal insights into disease pathogenesis. *Proc. Natl. Acad. Sci. U.S.A.* **110**, 10812–10817
42. Sato, N., and Morishita, R. (2015) The roles of lipid and glucose metabolism in modulation of β -amyloid, tau, and neurodegeneration in the pathogenesis of Alzheimer disease. *Front. Aging Neurosci.* **7**, 199
43. Miller, D. B. (1982) Neurotoxicity of the pesticidal carbamates. *Neurobehav. Toxicol. Teratol.* **4**, 779–787
44. Maddaiah, V. T., and Madsen, N. B. (1966) Kinetics of purified liver phosphorylase. *J. Biol. Chem.* **241**, 3873–3881
45. Cox, J., Hein, M. Y., Lubner, C. A., Paron, I., Nagaraj, N., and Mann, M. (2014) Accurate proteome-wide label-free quantification by delayed normalization and maximal peptide ratio extraction, termed MaxLFQ. *Mol. Cell Proteomics* **13**, 2513–2526
46. Cox, J., Neuhauser, N., Michalski, A., Scheltema, R. A., Olsen, J. V., and Mann, M. (2011) Andromeda: a peptide search engine integrated into the MaxQuant environment. *J. Proteome Res.* **10**, 1794–1805